PALEOECOLOGY, BIOEROSION, AND PALEOENVIRONMENTS IN THE LATE MIOCENE OF DAR PAHN UNIT, MAKRAN, SE IRAN

OLEV VINN ⓘ

Institute of Ecology and Earth Sciences, University of Tartu, Ravila 14A, 50411, Tartu, Estonia.
olev.vinn@ut.ee (Corresponding author)

MEHDI HADI ⓘ, DANGPENG XI ⓘ

State Key Laboratory of Biogeology and Environmental Geology, China University of Geosciences, Beijing, 100083, China.
mehdi_hadi_s@yahoo.com, 2011010027@cugb.edu.cn

MAJID MIRZAIE ATAABADI ⓘ

Department of Geology, Faculty of Sciences, University of Zanjan, Zanjan, 45137-66731, Iran. *majid.mirzaie@znu.ac.ir*

FRANCISCO J. VEGA ⓘ

Instituto de Geología, Universidad Nacional Autónoma de México, Ciudad Universitaria, Coyoacán, CDMX04510, Mexico.
vegver@unam.mx

ABSTRACT – This study focuses on sedimentation patterns and paleoecological conditions during the Upper Miocene in Southeast Iran, specifically analyzing the Rudig section. The sedimentation was predominantly terrigenous and occurred in marine conditions, forming multiple shallowing upwards sequences comprising silty marl, siltstone, and sandstone. The analysis of molluscan shells from this period indicates minimal bioerosion, with encrusters represented solely by *Balanus* sp. This low level of encrustation suggests rapid sedimentation and brief exposure times. Bioerosion was limited, with *Caulostrepsis taeniola* borings found only in the shells of vermetid *Thylacodes* sp. and predatory gastropod *Conus* sp. Predatory drillings, identified as *Oichnus paraboloides* were present in the shells of *Turritella* sp., *Corbula* sp., and *Bursa* sp., along with occasional shell aperture peeling repairs in *Turritella* sp. The presence of abundant large *Thalassinoides* burrows in the sandstone facies, along with moderate ichnodiversity supports the interpretation of the sandstone facies as shoreface. The rare occurrence of *Ophiomorpha nodosa* in siltstone facies, and the dominance of burrowing crustaceans in shallow water facies and suspension-feeding mollusks in deeper facies, provides further insight into the paleoenvironment. This study offers a detailed reconstruction of the sedimentary and ecological dynamics during the Upper Miocene in this region, enhancing our understanding of paleoenvironmental conditions and faunal interactions.

Keywords: biofacies, sedimentary facies, bioerosion, encrustation, predation, Cenozoic.

RESUMO – Este estudo enfoca os padrões de sedimentação e as condições paleoecológicas durante o Mioceno Superior no sudeste do Irã, analisando especificamente a seção Rudig. A sedimentação foi predominantemente terrígena, e ocorreu em condições marinhas, formando várias sequências de raseamento que compreendem marga siltosa, siltito e arenito. A análise das conchas de moluscos desse período indica bioerosão mínima, com incrustações representadas apenas por *Balanus* sp. Esse baixo nível de incrustação sugere sedimentação rápida e tempos de exposição breves. A bioerosão foi limitada, com perfurações de *Caulostrepsis taeniola* encontradas apenas nas conchas do vermetídeo *Thylacodes* sp. e do gastrópode predador *Conus* sp. Perfurações predatórias, identificadas como *Oichnus paraboloides*, estavam presentes nas conchas de *Turritella* sp., *Corbula* sp., e *Bursa* sp., juntamente com reparos ocasionais de descascamento da abertura da concha em *Turritella* sp. A presença abundante de grandes tocas de *Thalassinoides* na fácies de arenito, juntamente com a icnodiversidade moderada, apoia a interpretação da fácies de arenito de antepraia. A rara ocorrência de *Ophiomorpha nodosa* em fácies de siltito e a predominância de crustáceos escavadores em fácies de águas rasas e moluscos que se alimentam de suspensão em fácies mais profundas fornecem mais informações sobre o paleoambiente. Este estudo oferece uma reconstrução detalhada da dinâmica sedimentar e ecológica durante o Mioceno Superior nessa região, aprimorando nossa compreensão das condições paleoambientais e das interações faunísticas.

Palavras-chave: biofácies, fácies sedimentares, bioerosão, incrustação, predação, Cenozoico.

INTRODUCTION

The sclerobiont faunas of the Miocene and Cenozoic in general are similar to those of modern faunas (Taylor & Wilson, 2003). In the Miocene, encrusting and boring faunas were dominated by mollusks, bryozoans, polychaetes, and sponges (Taylor & Wilson, 2003; El-Hedeny, 2007; El-Sabbagh & El-Hedeny, 2016; El-Sabbagh *et al*., 2016; Salahi *et al*., 2018; Rashwan *et al*., 2019, 2022). Encrustation and bioerosion on hard substrates in the Miocene have been studied in detail by several authors (*e.g*., El-Hedeny, 2007; El-Sabbagh & El-Hedeny, 2016; El-Sabbagh *et al*., 2016; El-Hedeny & El-Sabbagh, 2018), but sclerobiont faunas from the Miocene of Iran have not received much attention. In contrast, encrustation patterns, bioerosion, and soft sediment trace fossils of the Miocene are well-known in some regions in the Middle East and Egypt (El-Hedeny, 2007; El-Sabbagh & El-Hedeny, 2016; El-Sabbagh *et al*., 2016; El-Hedeny & El-Sabbagh, 2018). The encrusting and bioeroding faunas of the Miocene of Iran have received little attention, especially compared with those of the Mediterranean region (El-Sabbagh & El-Hedeny, 2016; El-Sabbagh *et al*., 2016; El-Hedeny & El-Sabbagh, 2018). The Miocene localities in SE Iran are extensive and among the best localities in the region for the exposure and preservation of fossils.

The shells of mollusks constitute the most common organic hard substrates in tropical seas in the Cenozoic (Taylor & Wilson, 2003). Our knowledge of the Miocene mollusk fauna of Makran region from Iranian platform is poor, but several molluscan genera show a wide geographic distribution in the Miocene of Tethys Ocean. There is only a single report on the Miocene mollusks from Iran by Harzhauser *et al*. (2017). However, these authors studied Burdigalian (Lower Miocene) mollusk assemblages with emphasis on the findings of McCall *et al*. (1994) and Ghaedi *et al*. (2016) from the Band-e-Chaker units.

The goals of this paper are to (i) understand the nature of hard substrate fauna on mollusk shells from the Miocene of SE Iran; (ii) analyze soft sediment trace fossils in the Miocene of SE Iran; and (iii) discuss the paleoecology of the fossil assemblage, and paleoenvironments in the Miocene of SE Iran.

GEOLOGICAL BACKGROUND AND LOCALITY

The Iranian plateau was part of the Alpine-Himalayan orogeny and has been classically subdivided into eight sedimentary-structural provinces, each one characterized by a different geological history (Stöcklin, 1968). These are (from the north to the south): (1) the Kopet-Dagh Zone, NE Iran, (2) the Alborz Zone, N-NW Iran, (3) the Central Iranian Block or Cimmeria, consisting of three major continental blocks (Lut, Tabas, and Yazd) separated by major faults (Alavi, 1991), (4) the eastern Iranian suture zone, (5) the Urumieh-Dokhtar (Sahand-Bazman) magmatic arc, (6) the Zagros Zone, (7) the Sanandaj-Sirjan Zone, and (8) the Makran Zone (Figure 1A).

The Makran zone is one of the largest accretionary wedges in the world, about 350 km wide that is results from nearly N-S convergence between Arabia and Eurasia (*e.g*., DeMets *et al*., 2010) and grows both vertically and laterally by scraping and incorporating sediments of the subducting Arabian Plate lithosphere (Platt *et al*., 1985; Burg, 2018). This zone is known to have complex tectonic settings, being near the Triple Junction, where three tectonic plates (*i.e*., Eurasian, Indian, and Arabian) are interacting (*e.g*., Abbasi, 2020). Makran region is separated from the Zagros Mountain Belt to the west, by the dextral Minab-Zendan Transform Fault, and to the east, it is restricted by the sinistral Chaman Transform Fault System (Stöcklin, 1968; Bird *et al*., 1975).

The Makran accretionary complex developed throughout the Cenozoic in the convergent conditions as the result of the subduction of the oceanic part of the Arabian plate beneath Eurasia (Lut and Afghan blocks) (*e.g*., Byrne *et al*., 1992; Kopp *et al*., 2000; Haghipour, 2014). Makran accretionary zone contains four main provinces with different sedimentary and igneous rocks, reflecting different stages in the evolution of the accretionary wedge (Dolati, 2010) and these provinces include: (1) North Makran area, (2) Inner Makran, (3) Outer Makran, and (4) Coastal Makran.

The coastal region of Makran, situated between the Chah Khan Thrust to the north and the current coastline, contains a sedimentary sequence ranging from the Miocene to the Plio-Pleistocene periods (Burg, 2018). The Middle to Upper Miocene sequences occur in the synclines that form an arc-like pattern, visible as wide, "en échelon" structures, extending from the Minab-Zendan fault zone into Pakistan (Burg, 2018). Upper Miocene sandstones are largely derived from earlier Eocene to Lower Miocene deep-marine sediments of the Makran Basin (Burg, 2018). Gradual transitions from marl-dominated to calcareous sandstone-dominated units, spanning kilometers, indicate that finer sediments dominated in the south. The sedimentary sequences show the transition from mudstone-dominated to sandstone-dominated layers and are characterized by abundant bioturbation and marine gastropod shells, signifying the shift from shallow marine shelf to deltaic conditions. Bidirectional crossbedding suggests deposition in very shallow water and intertidal zones (Burg, 2018). There is also an olistostrome in the Miocene of Makran (Burg *et al*., 2008). A disordered, non-metamorphic formation characterized by a greenish muddy, shaly matrix lacking distinct internal stratigraphy or bedding, and containing randomly interspersed clasts of varying age, composition, shape, and size, exhibits structural and sedimentary characteristics typical of an olistostrome (Burg *et al*., 2008). This mass flow extended across the Inner, Outer, and Coastal Makran, spanning approximately 420 km from near the Iran-Pakistan border in the east to the Minab-Zendan fault zone in the west, and covering a north-south width of roughly 150 km. This would encompass an area of approximately 63,000 km². However, the submarine mass flow expanded within paleo-valleys around and between paleo-highs, initially not encompassing the entire region. Its
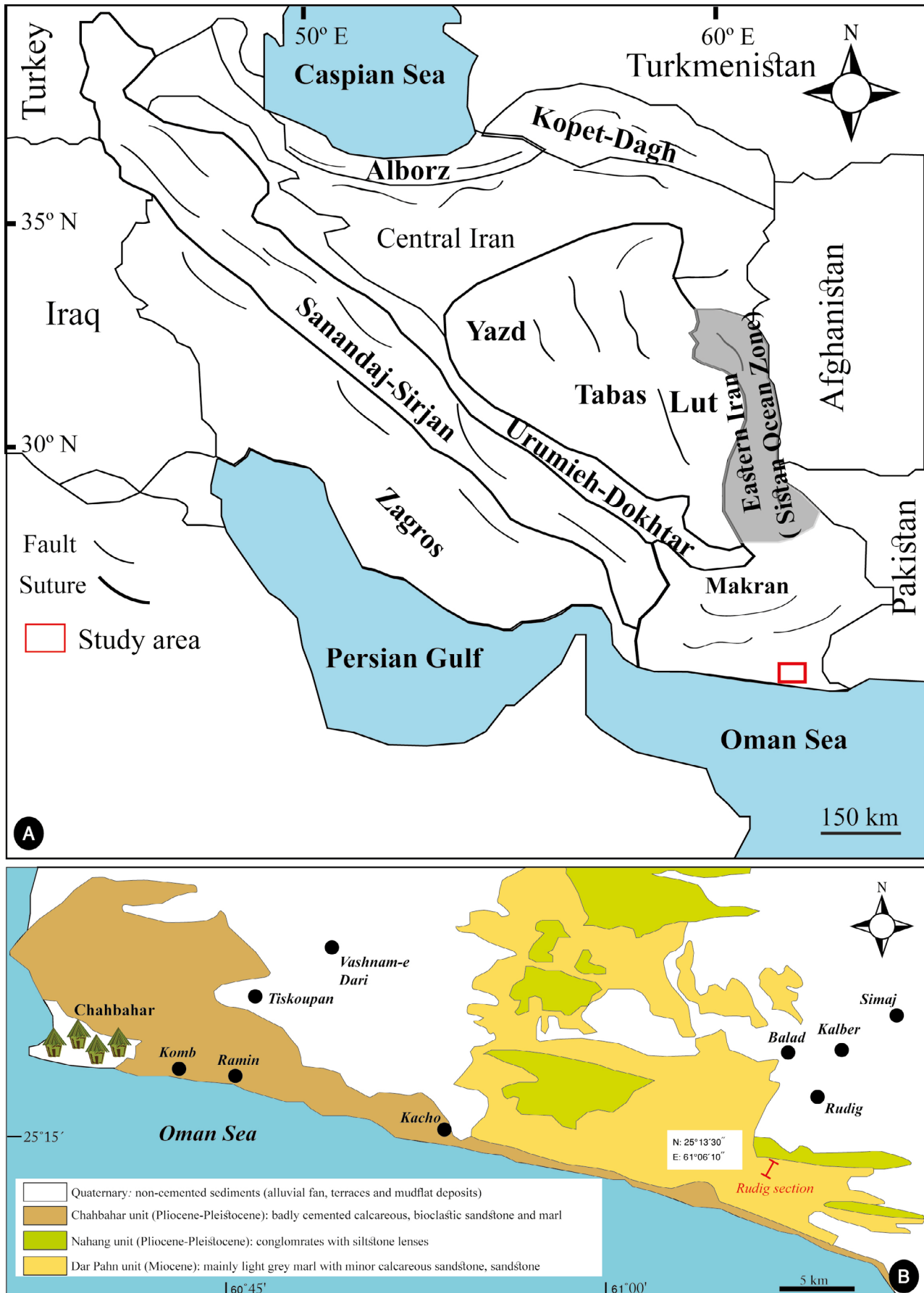
Figure 1. Location of Makran Zone (**A**) and study area (**B**) (modified after Stöcklin, 1968).

maximum estimated thickness reaches 600 m in paleo-valleys, tapering towards the south (Burg *et al.*, 2008).

The Rudig section is located about 6 km south of Rudig village, 50 km east of Chabahar (Figure 1B). The section has a total thickness of 100 m within the Coastal Makran area, and is composed of an alternation of sandstone, silty marl, marly limestone, and siltstone, which form together a "Dar Pahn" unit, *i.e.*, a formal lithological unit (McCall, 1985; Hadi *et al.*, 2024) (Figure 2). In previous studies, the deposits of the Dar Pahn unit are assigned to the Middle–Upper Miocene to Pliocene (McCall, 1985; Dolati, 2010). However, Hadi *et al.* (2024) assigned the age of the current study section to Lower Miocene (upper Aquitanian to lower Burdigalian), based on calcareous nannofossil biostratigraphy. The lower stratigraphic boundary of the unit is marked by the Chah Khan Thrust in the northern areas (approximately 70-80 km north of Rudig village), whereas the marl-dominated member is covered unconformably by the continental deposits of the Pliocene–Pleistocene Nahang Unit (Dolati, 2010). The Rudig section consists of three units: unit 1, with a Tortonian age, is composed of thin horizontal-bedded marly siltstone with subordinate thin to medium horizontal-bedded sandstone; unit 2 is an upward-thickening association of thin to medium-grained, well-sorted from siltstone to sandstone beds that were considered Tortonian in age. Unit 3 is characterized by a thin horizontal-bedded marl and silty marl intercalated with thin-medium beds of siltstone and sandstone during the Tortonian to early Messinian? age (Figure 2).

MATERIAL AND METHODS

This study is based on 371 specimens that were collected with 2–3 m sampling intervals composed of marl, silty marl, siltstone and sandstone beds containing abundant well-preserved mollusks specimens. Additionally, hundreds of field photographs were analyzed. Collected specimens were photographed uncoated with EOS2000D digital camera. Specimens are deposited at the paleontological collection of the Geology Department of Zanjan University, Iran, under the acronym GDZU.

RESULTS

Sedimentary facies

In the Rudig section, sediments are usually homogeneous, showing layering and only few sedimentary structures. Four sedimentary facies occur in the Rudig section: 1) sandstone facies (*i.e.*, light yellowish thin to medium horizontal-bedded sandstone, coarse to medium-grained, vertical shafts of *Thalassinoides*). The sandstones contain ovoid-shaped elongated nodules (Figure 3). The surface of sandstones shows a high degree of erosion. Bivalve casts and external molds are preserved on the sandstone surfaces; 2) siltstone facies (*i.e.*, light grey medium-grained well-sorted thin to medium horizontal-bedded siltstone, only horizontal shafts of *Thalassinoides*). There are spherical nodules with nuclei

of gastropods and bivalves from the siltstone horizons; 3) silty marl facies (*i.e.*, light grey thin horizontal-bedded silty marl, fine-grained). There are log-like structures with nuclei of vertebrate bones (*i.e.*, fossil whales) and bivalve shell beds with well-preserved shells in the silty marl facies; and 4) marl facies (*i.e.*, grey thin horizontal-bedded marl without any other sedimentary structures) (Figure 4). The sandstone and siltstone facies show high bioturbation levels by large *Thalassinoides* burrows. The bioturbation in the other three sedimentary facies was minor, as indicated by the presence of a few *Ophiomorpha nodosa* specimens in the siltstone facies. The mollusks are well-preserved in the siltstone and marl facies.

Soft substrate trace fossils

Thalassinoides horizontalis Myrow, 1995 (p. 72, figs. 6–9) (Figure 5A–D). The branching framework of smooth-walled, unlined horizontal burrows, lacking vertically oriented offshoots. Their burrow diameter is constant within individual specimens (62 to 96 mm); constrictions or swellings at both junctions and inter-junction segments are absent. This ichnospecies dominates but co-occurs with *Thalassinoides suevicus* (Rieth, 1932). Traces are preserved in the form of a wall, and the inner core is a finer sandstone filling in the sandstone matrix. The burrows were made for deposit-feeding and dwelling by crustaceans.

Thalassinoides suevicus (Figure 5E). The more or less regularly branched, mostly cylindrical components forming large burrow systems where dichotomous bifurcations are more common than T-shaped branches; swellings and chambers occur (Frey & Howard, 1985, p. 394). The burrow systems are predominantly horizontal. Traces are preserved in the form of a wall and the inner core is sandstone filling in the sandstone matrix. The diameter of the burrows is 10 to 12.4 mm. The burrows were made for deposit-feeding and dwelling by crustaceans.

Ophiomorpha nodosa Lundgren, 1891 (Figure 5G). The cylindrical burrow with pelleted lining. The wall of a horizontal burrow consists predominantly of dense, regularly distributed angular to ovoid pellets (Frey *et al.*, 1978). The burrow interior is more or less smooth. Occurs in siltstone facies. External diameter of the burrow is 38 mm. Trace is the dwelling burrows of decapod crustaceans.

Bioerosional trace fossils

Caulostrepsis taeniola Clarke, 1908 (Figure 6A–B). The elongate and narrow U-shaped boring with two merged circular apertures, distinct limbs, and an interconnecting vane. Common in vermetid *Thylacodes* sp.; rare in *Conus* sp. (N = 2). The diameter of the aperture is 1.4 to 2.0 mm. The trace is a domichnion. The boring is produced mainly by the polychaete *Polydora* (Hanken *et al.*, 2012).

Oichnus paraboloides Bromley, 1981 (Figure 6C–E). Simple single boring with circular outline completely penetrating the shell wall. The diameter of the boring at the external surface is slightly larger than the diameter at the internal surface of the shell wall. The external diameter is
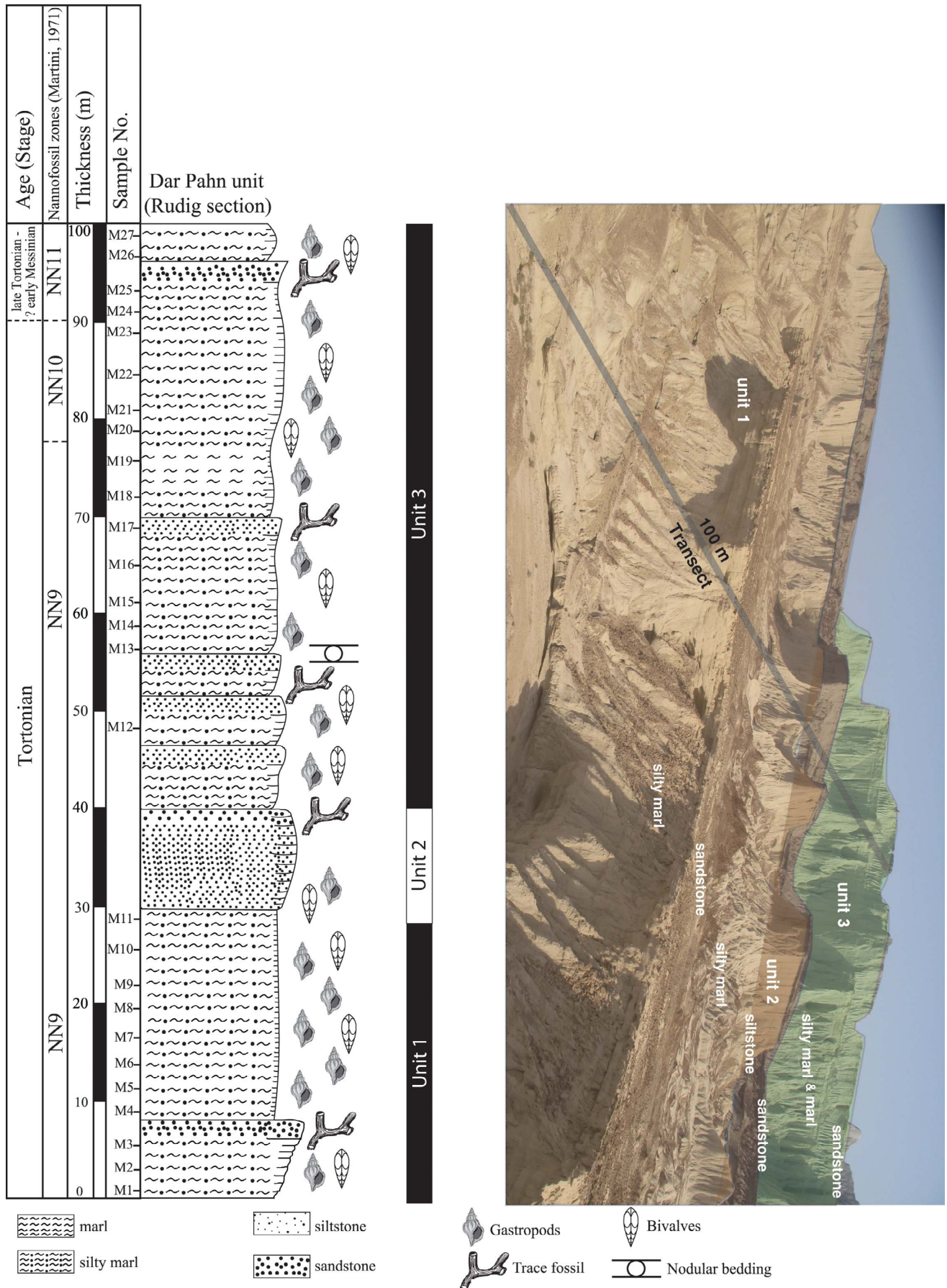
Figure 2. Stratigraphy of the Rudig section. **A**, lithostratigraphic log of the Dar Pahn Unit (Ruding section). **B**, panoramic view of the studied succession.

Figure 3. Ovoid-shaped nodules in the sandstone facies.
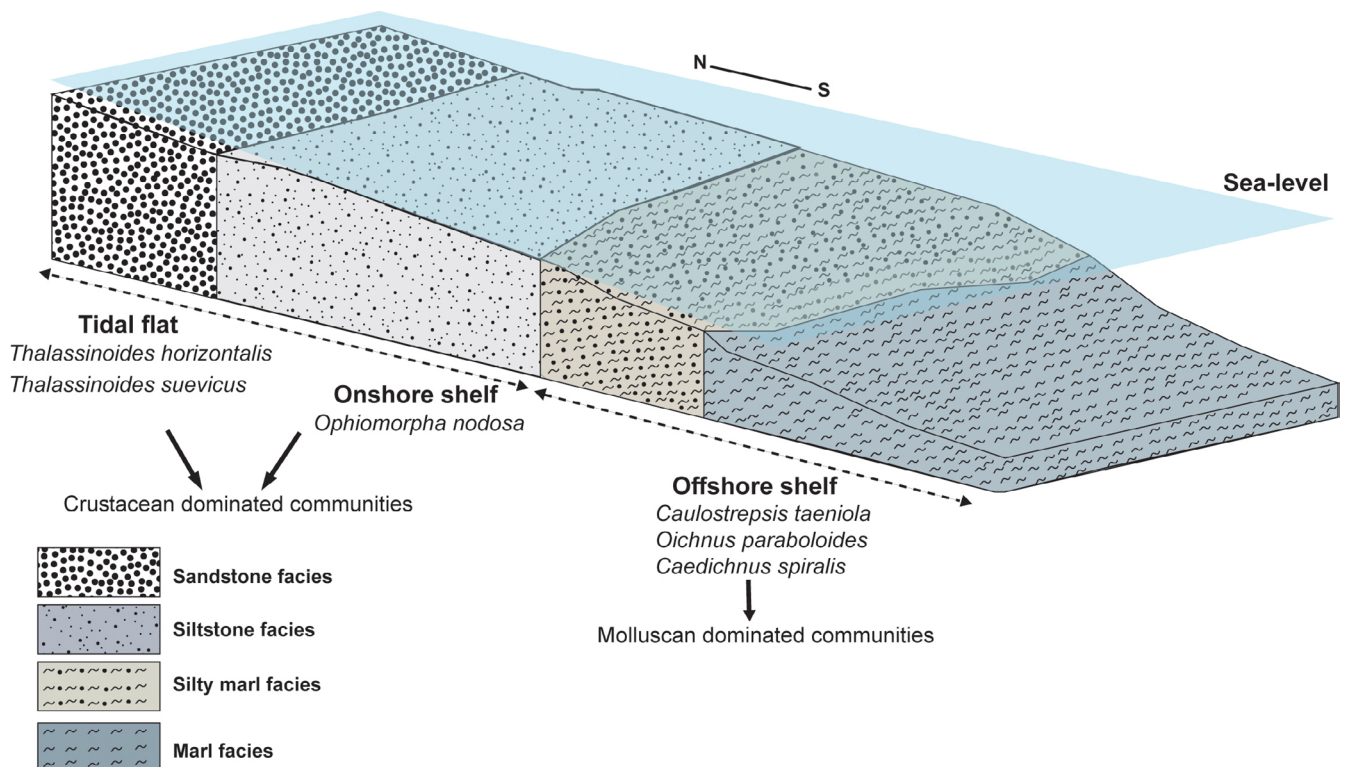

Figure 4. Facies model of the Dar Pahn Unit, Late Miocene of SE Iran.

1.1 to 1.2 mm. It occurs in a few specimens (3 of 53 shells collected) of *Turritella* sp., in a single specimen of *Corbula* sp. (25 shells collected), and of *Bursa* sp. (89 shells collected) in silty marl facies. The borings were made by predatory gastropods.

Caedichnus spiralis Stafford *et al*., 2015 (Figure 6F). Repaired marks of shell aperture peeling occur in a few shells (N = 2 of 53 shells collected) of *Turritella* sp. In the adult shell part. The trace is as wide as the affected gastropod whorl (8.0 mm). This trace of gastropod aperture peeling occurs in silty marl facies. Traces were made by shell-peeling predators.

Balanus sp. (Figure 6G–I). Several *Pecten* sp. shells and a single gastropod show encrustation by multiple specimens of *Balanus* sp. The encrustation cover varies greatly; some shells have only a few *Balanus* sp., whereas others are densely covered in large portions. The encrustation occurs preferentially on shell exteriors, but some interiors are also encrusted. This encrustation occurs in silty marl facies.

The identification of mollusks was based on the systematic paper by Hadi *et al*. (2024). The gastropod fauna includes: *Turritella* sp., *Thylacodes* sp., *Polinices* sp., *Tibia* sp., *Bursa* sp., *Bullia* sp., *Mitra* sp., *Conus* sp., *Leucosyrinx* sp., and *Architectonica* sp. The bivalve fauna includes *Anadara* sp., *Ostrea* sp., *Pecten* sp., *Anomia* sp., *Dosinia* sp., *Pophia* sp., *Tagelus* sp., and *Corbula* sp.

All bivalves (*i.e.*, *Ostrea*, *Pecten*, *Anomia*, *Pophia*, *Corbula*, *Dosinia*, *Tagelus*, *Anadara*) and the gastropod *Turritella* were suspension feeders (Heller, 2015). Among gastropods, predatory life mode was most common (*i.e.*, *Mitra*, *Conus*, *Leucosyrinx*, *Bursa*, *Polinices*) (Heller, 2015). Among predators, *Ploinices* was a boring predator. Scavengers were represented by *Bullia* and omnivores by *Tibia*, whereas mucus net feeding occurred in *Thylacode*s (Heller, 2015).

DISCUSSION

Reconstruction of sedimentary environment

The sedimentation was dominantly terrigenous and occurred in a low-energy environment, as indicated by horizontal bedding. The section contains multiple shallowing upward sequences (*i.e.*, silty marl-siltstone-sandstone). Most regressions were gradual, whereas the following transgressive events were sudden, as indicated by the change in grain size. The alternating regressions and transgressive events were likely due to regional small-scale tectonic movements (Byrne *et al*., 1992; Kopp *et al*., 2000). Sandstones formed close to the shore in shallowest water conditions, followed by siltstones in the offshore direction. Both sandstone and siltstone facies were typical shallow water shoreface environments (Figure 4). On one hand, the waters in the sandstone facies may have been too turbulent for the molluscan fauna. On the other hand, such turbulence could have destroyed entirely molluscan shells. The same could be true for the siltstone facies. However, silt is usually deposited in calmer conditions than sand, and the complete destruction of molluscan shells

seems unlikely. Thus, it is possible that mollusks preferred deeper offshore regions of the shelf in the Late Miocene of SE Iran. Alternatively, siltstones could be deposited in the tidal flat, which is a harsh subenvironemnt for mollusks, but this interpretation is not supported by sedimentary structures.

Silty marls and marls formed in the deeper offshore region of the shelf (Figure 4), presumably still in the photic zone, as indicated by the presence of shallow-water mollusks. Some molluscan shells are large and fragile enough, such as *Ostrea* sp. and *Pecten* sp., suggesting they were autochthonous, while the smaller molluscan shells could also be transported by storm events from the shallower regions of the basin (*i.e.*, sandstone and siltstone facies), though their excellent state of preservation rather suggests a burial without major transportation and there is no HCS or other oscillatory flows evidence. Complete and articulated bivalve shells such as *Anadara* sp., *Dosinia* sp., and *Corbula* sp. clearly represent autochthonous assemblages. The influence of waves was low as the molluscan shells are, in general, well-preserved, but thin shell-beds occur, and there are no sedimentary structures indicative of strong wave activity. Thus, the waters were occasionally hydrodynamically active enough to allow thin shell accumulations to form.

Ichnology

The ichnospecies diversity of *Thalassinoides* is moderate in the sandstone facies as compared to similar occurrences in the Miocene (El-Sabbagh *et al*., 2017). The presence of abundant large *Thalassinoides* burrows in the sandstone and siltstone facies indicates that the seafloor was well-oxygenated and burrowing invertebrates could thrive in the sediments of the sea floor. *Thalassinoides* does not represent a shallow burrow, but burrows produced at depth of 0.5 m or more in lagoons, and 0.7 m or more in shallow seas. Thus, the sediments of the sea floor were likely well-oxygenated. There is no doubt that *Thalassinoides* trace makers are gebiid (thalassinid) crustaceans (Knaust, 2024). The size of the burrows indicates that the thalassinid crustaceans had a large size. The abundance of *Thalassinoides* could be explained by the ecological pressure of *Thalassinoides* trace-makers (El-Sabbagh *et al*., 2017). *Thalassinoides* has a wide environmental distribution (Frey *et al*., 1978) and is usually reported in shallow facies (mainly in the Paleozoic and Mesozoic) to very deep environments in the Cenozoic (*e.g.*, Bromley, 1990; Fürsich, 1998; Uchman, 1998; Giannetti & Monaco, 2004). Modern *Thalassinoides* burrows are common in intertidal flats (Howard & Frey, 1975; Letzsch & Frey, 1980). However, they also occur in shallow marine settings, maybe even in deeper marine settings, as their trace makers occupied all these habitats. Considering the abundance of *Thalassinoides* in modern and ancient shoreface settings, the interpretation of sandstone facies of Rudig section as a shoreface seems plausible. Substrate consistency is an important factor controlling the distribution of *Thalassinoides* in marine environments (*e.g.*, Myrow, 1995; Pemberton *et al*., 2004; Mikuláš, 2006). *Thalassinoides* is most common in softgrounds, although they can occur in firmgrounds

Figure 5. A, Accumulation of shells of mollusks on the bedding plane, silty marl facies. **B–D, F**, *Thalassinoides horizontalis* Myrow, 1995 from sandstone facies. **E**, *Thalassinoides suevicus* (Rieth, 1932) from sandstone facies. **G**, *Ophiomorpha nodosa* Lundgren, 1891 from siltstone facies.

Figure 6. A–B, *Caulostrepsis taeniola* Clarke, 1908 borings in *Conus* sp. from silty marl facies. **C–D**, *Oichnus paraboloides* Bromley, 1981 in multiple *Turritella* sp. specimens from silty marl facies. **E**, Single *Oichnus paraboloides* Bromley, 1981 predatory drilling in *Corbula* sp. from silty marl facies. **F**, *Caedichnus spiralis* Stafford *et al*., 2015 in *Turritella* sp. from silty marl facies. **G**, multiple encrusting *Balanus* sp. on a gastropod specimen from silty sandstone facies. **H**, multiple encrusting *Balanus* sp. on a bivalve fragment. **I**, multiple encrusting *Balanus* sp. on *Pecten* sp. from silty sandstone facies. Scale bars: A–D, F = 5 mm; E = 2 mm; G = 10 mm; H–I = 20 mm.

(Pemberton *et al*., 2004; El-Sabbagh *et al*., 2017; Bendella *et al*., 2021). We interpret the sandstone facies of Rudig section as a softground.

The absence of abundant worm burrows in silty marl facies and marl facies needs an explanation. Fast sedimentation in silty marl and marl facies could have been among the reasons why the levels of bioturbation were low. Oxygen deficiency seems possible as the sea floor inhabited by a rich assemblage of gastropods and bivalves could be oxygenated, but the substrates could have been dysoxic or anoxic.

Both *Ophiomorpha* and *Thalassinoides* are crustacean burrows, indicating that, in addition to the abundant mollusks, crustaceans were also common in the Upper Miocene of SE Iran.

Paleoecology of the fossil assemblage at Rudig section

Shallow water facies were dominated by crustaceans' burrows (*Thalassinoides* and *Ophiomorpha*) and deeper facies were dominated by mollusks (Figure 4). Modern decapod crustaceans are among the dominant macrobenthos dwellers in tropical shoreface settings (Reise, 1991; Dittmann, 1995) and the here studied *Thalassinoides*-rich sand facies is very similar to recent tropical shoreface. The mollusk association was dominated by suspension feeders that included all bivalve species, single gastropods, and crustaceans (*i.e*., *Balanus* sp.). The abundance of suspension feeders in silty marl and marl facies of a shallow tropical sea is not surprising in the Cenozoic, but it is weird that no trace fossils were found in a place that was dominated by suspension-feeding organisms (Gili & Coma, 1998). However, the abundance of predatory snails is striking. The abundance of predators also indicates the assemblage likely contained numerous soft-bodied prey species that were not preserved as fossils. The absence of trails is difficult to explain, whereas the absence of burrows could result from oxygen deficiency in the sediments. The occurrence of the naticid gastropod *Polinices* might explain the borings in the other gastropods (*i.e*., *Turritella* sp.) and bivalves (*i.e*., *Corbula* sp.). However, the number of bored mollusk shells is rather low, considering the presence of naticids in the association. In the past, laboratory trials have shown that all prey consumed by *Polinices* were drilled (Kitchell *et al*., 1981). However, some prey (*e.g*., *Ensis*) could be taken without drilling (Edwards & Huebner, 1977). This situation can be explained either by naticids taking prey without drilling or, alternatively, their abundance was low in the community.

The encrustation of mollusk shells is also rather not intense for a tropical shallow sea in the Miocene (Taylor & Wilson, 2003; El-Hedeny, 2007; El-Sabbagh & El-Hedeny, 2016; El-Sabbagh *et al*., 2016; Salahi *et al*., 2018; Rashwan *et al*., 2019, 2022). Moreover, the encrusters were represented only by barnacles and vermetid gastropods, though the latter were all found unattached. The low encrustation levels usually indicate rather fast sedimentation and short exposure times.

However, the occurrence of bioerosion does not support fast sedimentation. Alternatively, the lack of sclerobionts may indicate that shell surfaces were preoccupied with some soft-bodied, fast-growing epibionts or that a salinity stress prevented certain epibionts from colonizing the shells. The occurrence of barnacle encrustation on shell exteriors suggests that *Balanus* sp. likely colonized living bivalves. The rarity of bioeroded shells in the Rudig section supports the idea of fast sedimentation and burial in the silty marl facies. Especially surprising is the lack of sponge borings (*i.e*., *Entobia*), which are one of the most common bioerosional traces in the Cenozoic shells in the region (El-Hedeny, 2007; El-Hedeny & El-Sabbagh, 2018; Salahi *et al*., 2018; Rashwan *et al*., 2019, 2022). The lack of *Entobia* presumably indicates the absence of boring sponges in the Rudig section association because, if the exposure time was long enough for *Caulostrepsis* to form, then there would have been enough time for sponges to produce borings. The lack of sponges may indicate salinity stress.

CONCLUSIONS

The sedimentation in the Upper Miocene of Southeast Iran was primarily terrigenous and occurred in marine conditions. The trace fossils suggest an impacted environment, potentially by salinity changes or high energetic storms, while the general body fossils are also not that diverse and dominated by mollusks. Within the Rudig section, there are several sequences with the transition from silty marl to siltstone and then to sandstone, indicating shallowing upwards patterns.

Bioerosion is infrequently observed in molluscan shells, indicating a short exposure time on the seafloor. Encrustation is mainly attributed to *Balanus* sp., suggesting relatively rapid sedimentation and brief exposure periods. Predatory boring in shells indicate presence of numerous predators in the ecosystem of Rudig section.

Thalassinoides burrows are abundant in sandstone facies, indicating a moderate ichnospecies diversity compared to similar occurrences in the Miocene. The interpretation of sandstone facies in the Rudig section as a shoreface appears plausible. Burrowing crustaceans dominated shallow water facies similarly to many modern tropical shoreface settings, while suspension-feeding mollusks prevailed in deeper facies.

REFERENCES

Abbasi, M.I.H. 2020. Is Makran A Separate Microplate? A Short Review. *Malaysian Journal of Geosciences*, **5**:1–5. *doi:*10.26480/mjg.01.2021.01.05

Alavi, M. 1991. Sedimentary and structural characteristics of the Paleo-Tethys remnants in northeastern Iran. *American Journal of Science*, **304**:1–20. *doi:*10.1130/0016-7606(1991)103%3C0 983:SASCOT%3E2.3.CO;2

Bendella, M.; Benyoucef, M.; Mikuláš, R.; Bouchemla, I.; Martinell, J. & Ferré, B. 2021. Shallow to marginal marine ichnoassemblages from the Upper Pliocene Slama Formation (Lower Chelif Basin, NW Algeria). *Geologica Carpathica*, **72**:529–548. *doi:*10.31577/GeolCarp.72.6.5

Bird, P.; Toksoz, M.N. & Sleep, N.H. 1975. Thermal and mechanical models of continent convergence zones. *Journal of Geophysical Research, Solid Earth*, **80**:4405–4416. *doi:*10.1029/JB080i032p04405

Bromley, R.G. 1981. Concepts in ichnology illustrated by small round holes inshells. *Acta Geológica Hispánica*, **16**:55–64.

Bromley, R.G. 1990. *Trace Fossils: Biology and Taphonomy*. Special Topics in Paleontology. London, Unwin Hyman Ltd, 281 p.

Burg, J.-P. 2018. Geology of the onshore Makran accretionary wedge: Synthesis and tectonic interpretation. *Earth-Science Reviews*, **185**:1210–1231. *doi:*10.1016/j.earscirev.2018.09.011

Burg, J.-P.; Bernoulli, D.; Smit, J.; Dolati, A. & Bahroudi, A. 2008. A giant catastrophic mud-and-debris flow in the Miocene Makran. *Terra Nova*, **20**:188–193. *doi:*10.1111/j.1365-3121.2008.00804.x

Byrne, D.E.; Sykes, L.R. & Davis, D.M. 1992. Great thrust earthquakes and aseismic slip along the plate boundary of the Makran subduction zone. *Journal of Geophysical Research, Solid Earth*, **97**:449–478. *doi:*10.1029/91JB02165

Clarke, J.M. 1908. The beginnings of dependent life. *New York State Museum Bulletin*, **121**:149–169.

DeMets, C.; Gordon, R.G. & Argus, D.F. 2010. Geologically current plate motions. *Geophysical Journal International*, **181**:1–80. *doi:*10.1111/j.1365-246X.2009.04491.x

Dittmann, S. 1995. Benthos structure on tropical tidal flats of Australia. *Helgoländer Meeresunters*, **49**:539–551.

Dolati, A. 2010. *Stratigraphy, structural geology and low-temperature thermochronology across the Makran accretionary wedge in Iran*. Eidgenössische Technische Hochschule Zürich, Ph.D. Thesis, 309 p.

Edwards, D.C. & Huebner, J.D. 1977. Feeding and growth rates of *Polinices duplicatus* preying on Mya arenaria at Barnstable Harbor, Massachusetts. *Ecology*, **58**:1218–1236. *doi:*10.2307/1935077

El-Hedeny, M. 2007. Encrustation and bioerosion on Middle Miocene bivalve shells and echinoid skeletons: paleoenvironmental implications. *Revue de Paléobiologie*, **26**:381–389.

El-Hedeny, M. & El-Sabbagh, A. 2018. *Entobia* ichnofacies from the Middle Miocene carbonate succession of the northern Western Desert of Egypt. *Annales Societatis Geologorum Poloniae*, **88**:1–19. *doi:*10.14241/asgp.2018.002

El-Sabbagh, A.M. & El-Hedeny, M.M. 2016. A shell concentration of the Middle Miocene *Crassostrea gryphoides* (Schlotheim, 1813) from Siwa Oasis, Western Desert, Egypt. *Journal of African Earth Sciences*, **120**:1–11. *doi:*10.1016/j.jafrearsci.2016.04.007

El-Sabbagh, A.; El-Hedeny, M. & Al Farraj, S. 2017. *Thalassinoides* in the Middle Miocene succession at Siwa Oasis, northwestern Egypt. *Proceedings of the Geologists' Association*, **128**:222–233. *doi:*10.1016/j.pgeola.2017.01.001

El-Sabbagh, A.M.; El-Hedeny, M.M.; Rashwan, M.A. & Abdel Aal, A.A. 2016. The bivalve *Placuna* (*Indoplacuna*) *miocenica* from the Middle Miocene of Siwa Oasis, Western Desert of Egypt: systematic paleontology, paleoecology, and taphonomic implications. *Journal of African Earth Sciences*, **116**:68–80. *doi:*10.1016/j.jafrearsci.2015.12.022

Frey, R.W. & Howard, J.D. 1985. Trace fossils from the Panther Member, Star Point Formation (Upper Cretaceous), Coal Creek Canyon, Utah. *Journal of Paleontology*, **59**:370–404.

Frey, R.W.; Howard, J.D. & Pryor, W.A. 1978. *Ophiomorpha*: its morphologic, taxonomic, and environmental significance. *Palaeogeography, Palaeoclimatology, Palaeoecology*, **23**:199–229. *doi:*10.1016/0031-0182(78)90094-9

Fürsich, F.T. 1998. Environmental distribution of trace fossils in the Jurassic of Kachchh (Western India). *Facies*, **39**:243–272. *doi:*10.1007/BF02537019

Ghaedi, M.; Johnson. K. & Yazdi, M. 2016. Paleoenvironmental conditions of Early Miocene corals, western Makran, Iran. *Arabian Journal of Geosciences*, **9**:686. *doi:*10.1007/s12517-016-2712-3

Giannetti, A. & Monaco, P. 2004. Burrow decreasing upward parasequence (BDUP): a case study from the Lower Jurassic of the Trento carbonate platform (Southern Alps), Italy. *Rivista Italiana di Paleontologia e Stratigrafia*, **110**:77–85. *doi:*10.13130/2039-4942/6267

Gili, J.-M. & Coma, R. 1998. Benthic suspension feeders: their paramount role in littoral marine food webs. *Trends in Ecology and Evolution*, **13**:316–321.

Hadi, M.; Mirzaie Ataabadi, M.; Sharifi, J.; Parandavar, M.; Castillo-Rodríguez, Z.G.; Vega-Sandoval, F.A. & Vega, F.J. 2024. Late Miocene Mollusca from the Dar Pahn unit, Makran, SE Iran. *Boletin de la Sociedad Geologica Mexicana*, **76**:1–22. *doi:*10.18268/BSGM2024v76n1a091223

Haghipour, N. 2014. *Active deformation and landscape evolution of the Makran Accretionary Wedge (SE-Iran). New constraints from surface exposure dating of fluvial terraces*. Eidgenössische Technische Hochschule Zürich, Ph.D. Thesis, 165 p.

Hanken, N.M.; Uchman, A. & Jakobsen, S.L. 2012. Late Pleistocene-early Holocene polychaete borings in NE Spitsbergen and their palaeoecological and climatic implications: An example from the Basissletta area. *Boreas*, **41**:42–55. *doi:*10.1111/j.1502-3885.2011.00223.x

Harzhauser, M.; Reuter, M.; Mohtat, T. & Piller, W.E. 2017. Early Miocene reef-and mudflatassociated gastropods from Makran (SE-Iran). *Paläontological Zeitzschrift*, **91**:519–539. *doi:*10.1007/s12542-017-0354-8

Heller J. 2015. *Sea snails: a natural history*. Springer Cham,354 p.

Howard, J.D. & Frey, R.W. 1975. Estuaries of Georgia coast, U.S.A.: Sedimentology and Biology, II. Regional animal-sediment characteristics of Georgia estuaries. *Senckenbergiana Maritima*, **4**:125–167.

Kitchell, J.A.; Boggs, C.H.; Kitchell, J.F. & Rice, J.A. 1981. Prey selection by naticid gastropods: experimental tests and application to application to the fossil record. *Paleobiology*, **7**:533–552. *doi:*10.1017/S0094837300025574

Knaust, D. 2024. The trace fossil *Thalassinoides paradoxicus* Kennedy, 1967 revisited from its type locality (Albian-Cenomanian chalk, SE England). *Palaeogeography, Palaeoclimatology, Palaeoecology*, **634**:111913. *doi:*10.1016/j.palaeo.2023.111913

Kopp, C.; Fruehn, J.; Flueh, E.R.; Reichert, C.; Kukowski, N.; Bialas, J. & Klaeschen, D. 2000. Structure of the Makran

subduction zone from wide-angle and reflection seismic data. *Tectonophysics*, **329**:171–191. *doi:*10.1016/S0040-1951(00)00195-5

Letzsch, W.S. & Frey, R.W. 1980. Deposition and erosion in a Holocene salt marsh, Sapelo Island, Georgia. *Journal of Sedimentary Petrology*, **50**:529–542. *doi:*10.1306/212F7A45-2B24-11D7-8648000102C1865D

Lundgren, B. 1891. Studier öfver fossilförande lösa block. *Geologiska Föreningens i Stockholm Förhandlingar*, **13**:111–121.

McCall, G.J.H. 1985. *East Iran Project-Area No: 1.* Geological Survey of Iran, Report 57, 636 p.

McCall, J.; Rosen, B. & Darrell, J. 1994. Carbonate deposition in accretionary prism settings: Early Miocene coral limestones and corals of the Makran Mountain Range in southern Iran. *Facies*, **31**:141–177. *doi:*10.1007/BF02536938

Mikuláš, R. 2006. Ichnofabric and substrate consistency in Upper Turonian carbonates of the Bohemian Cretaceous Basin (Czech Republic). *Geologica Carpathica*, **57**:79–90.

Myrow, P.M. 1995. *Thalassinoides* and the enigma of Early Paleozoic open framework burrow systems. *Palaios*, **10**:58–74. *doi:*10.2307/3515007

Pemberton, S.G.; MacEachern, J.A. & Saunders, T. 2004. Stratigraphic applications of substrate-specific ichnofacies: delineating discontinuities in the rock record. *In*: D. McIlroy (Ed.) *The Application of Ichnology to Palaeoenvironmental and Stratigraphic Analysis*, Special Publication 228, Geological Society of London, p. 29–62.

Platt, J.P.; Leggett, J.K.; Young, J.; Raza, H. & Alam, S. 1985. Large-scale sediment underplating in the Makran accretionary prism, southwest Pakistan. *Geology*, **13**:507–511 *doi:*10.1130/0091-7613(1985)13%3C507:LSUITM%3E2.0.CO;2

Rashwan, M.; El-Sabbagh, A.; El Hedeny, M.; Vinn, O. & Mansour, H. 2022. Taphonomy and its significant role in palaeoenvironmental reconstruction of the upper Turonian actaeonellid gastropod concentrations of Abu Roash, Western Desert, Egypt. *Lethaia*, **55**:1–18. *doi:*10.18261/let.55.1.8

Rashwan, M.; Vinn, O.; El Hedeny, M. & Jäger, M. 2019. Sclerobiont assemblages on the late Eocene bivalve *Carolia placunoides*: composition, distribution and their paleoecological significance. *Proceedings of the Geologists Association*, **130**:612–623. *doi:*10.1016/j.pgeola.2019.06.002

Reise, K. 1991. Macrofauna in mud and sand of tropical and temperate tidal flats. *In*: M. Elliott & J.P. Ducrotoy (eds.) *Estuaries and coasts: spatial and temporal intercomparisons*, Olsen and Olsen, p. 211–216.

Rieth, A. 1932. Neue Funde Spongeliomorpher Fucoiden aus dem Jura Schwabens. *Geologische und Paläontologische Abhandlungen*, **19**:257–294.

Salahi, A.; El Hedeny, M.; Vinn, O. & Rashwan, M. 2018. Sclerobionts on organic substrates from the Late Paleocene Chehel-Kaman Formation, Kopet- Dagh Basin, NE Iran. *Annales Societatis Geologorum Poloniae*, **88**:291–301. *doi:*10.14241/asgp.2018.022

Stafford, E.S.; Dietl, G.P.; Gingras, M.P. & Leighton, L.R. 2015. *Caedichnus*, a new ichnogenus representing predatory attack on the gastropod shell aperture. *Ichnos*, **22**:87–102. *doi:*10.1080/10420940.2015.1031899

Stöcklin, J. 1968. Structural history and tectonics of Iran: a review. *American Association of Petroleum Geologists Bulletin*, **52**:1229–1258.

Taylor, P.D. & Wilson, M.A. 2003. Palaeoecology and evolution of marine hard substrate communities. *Earth-Science Reviews*, **62**:1–103. *doi:*10.1016/S0012-8252(02)00131-9

Uchman, A. 1998. Taxonomy and ethology of flysch trace fossils: a revision of the Marian Ksiazkiewicz collection and studies of complementary material. *Annales Societatis Geologorum Poloniae*, **68**:105–218.